

# Flavonoids and flavonoid glycosides as natural weapons against virus replication. Theoretical approach on influenza and SARS-CoV-2

Daniel I. Hădărugă

Department of Applied Chemistry, Organic and Natural Compounds Engineering, Polytechnic University of Timișoara, 300001-Timișoara, Carol Telbisz 6, România

---

## Abstract

Flavonoids and flavonoid glycosides are natural antioxidants having various biological activities. Among these, the inhibition of enzymes responsible for virus replication is widely studied. The goal of the study was to evaluate the correlation of the inhibition effect of flavonoids, flavonoid glycosides and some auronones against AH1N1 and AH3N1 virus replication and extending the results for evaluating the inhibition effect on the SARS-CoV-2 enzymatic activity. Twenty-five compounds were subjected to molecular modeling and conformational analysis in order to obtain structural parameters that were correlated with the neuraminidase or polymerase inhibitory activities (QSARs). The best QSARs were obtained using the average Broto-Moreau autocorrelation and 3D topological distance based autocorrelation parameters, with correlation coefficients for inhibitory activity against AH1N1 neuraminidase of  $r = 0.792$  (AATS6v parameter) or  $r = 0.838$  (TDB6m parameter), and against AH3N2 polymerase of  $r = 0.714$  for TDB5m parameter. The most active compounds were evaluated for their efficacy on the interaction with SARS-CoV-2 protease using docking experiments. The best results were obtained with an aurone structure, (2E)-6-hydroxy-2-[(4-hydroxyphenyl)methylidene]-1-benzofuran-3(2H)-one. As a conclusion, these natural derivatives can be good candidates for evaluating the inhibition effect against SARS-CoV-2 replication.

**Keywords:** flavonoid, flavonoid glycosides, auronones, virus replication, SARS-CoV-2, coronavirus, influenza, neuraminidase, polymerase, proteinase, molecular modeling and docking

---

## 1. Introduction

Several pandemics have been reported in the last two decades, some of them due to influenza viruses. The AH1N1 virus generated the pandemic in 2009. It appears to be similar to the virus that caused the 1918 pandemic, which determined more than 100 million of deaths. Similar pandemics or epidemics related to AH1N1 or similar viruses appeared in 1957 and 1976, including AH3N2 [1-5].

The most recent pandemics is related to SARS-CoV-2 (severe acute respiratory syndrome coronavirus 2) [6,7]. It causes the coronavirus disease 2019 (COVID-19).

The way of infection by AH1N1 virus involves hemagglutinin, while the neuraminidase is

responsible for delivering of the virus into the human cell. Other enzymes such as polymerases PB1 and PB2 are responsible for replication and transcription of the viral information [8]. On the other hand, SARS-CoV-2 bind to the human cell through spike protein, S, by angiotensin converting enzyme 2 (ACE2) and further delivering into the cell. Cathepsin, a protease, is further responsible for virus release and then the replication of the virus into the cell [6,7].

Among many biologically active compounds investigated for their capability to inhibit various enzyme activities that are involved in the influenza and SARS-CoV-2 infection or replication, flavonoids are very promising. Studies on the inhibitory activity against neuraminidases and polymerases of AH1N1 and AH3N2 viruses have

---

\* Corresponding author: [daniel.hadaruga@upt.ro](mailto:daniel.hadaruga@upt.ro)

been performed in the case of well-known flavonoids, flavonoid glycosides, isoflavonoids and aurones [9]. The above-mentioned enzymes are involved in the catalysis of neuraminic acid, facilitating the transfer of the virus into the respiratory tract and the replication of the virus, respectively [9].

The goal of the study was to evaluate the correlation of the inhibition effect of flavonoids, flavonoid glycosides, isoflavonoids and some aurones against AH1N1 and AH3N1 virus replication and extending the results, for the first time, on evaluating the

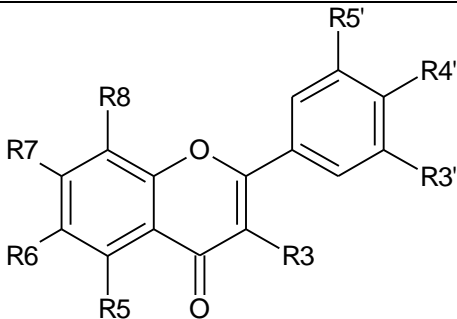
inhibition effect on the SARS-CoV-2 enzymatic activity.

## 2. Materials and Method

### 2.1. Selection of compounds

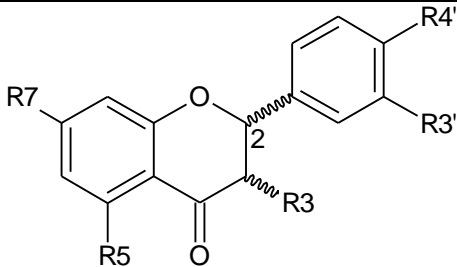
Flavonoids, flavonoid glycosides, isoflavonoids and aurones were selected from literature [9]. They had inhibitory activity against AH1N1 neuraminidase and AH3N2 polymerase, with  $pIC_{50}$  values of <4.0 to 4.66 for both cases (Tables 1-3).

**Table 1.** Flavonoid and flavonoid glycoside (flavone and flavonol subgroups) structures and their inhibitory activity against AH1N1 neuraminidase and AH3N2 polymerase [9]



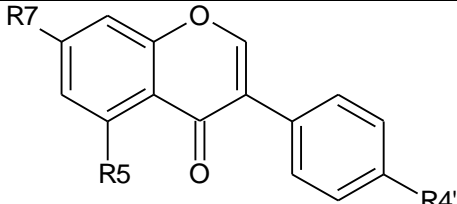
	R3	R5	R6	R7	R8	R3'	R4'	R5'	$pIC_{50}(AH1N1)$	$pIC_{50}(AH3N2)$
01_Apigenin	H	OH	H	OH	H	H	OH	H	4.50	4.54
02_Luteolin	H	OH	H	OH	H	OH	OH	H	4.47	4.49
03_Dinatin	H	OH	OMe	OH	H	H	OH	H	4.33	4.59
04_Scutellarin	H	OH	OH	OH	H	H	OH	H	4.30	4.33
05_Galuteolin	H	OH	H	OGlc	H	OH	OH	H	4.32	4.28
06_Vitexin	H	OH	H	OH	OGlc	H	OH	H	4.33	4.35
07_Chrysin	H	OH	H	OH	H	H	H	H	4.34	4.48
08_Kaempferol	OH	OH	H	OH	H	OH	OH	H	4.23	4.42
09_Quercetin	OH	OH	H	OH	H	OH	OH	H	4.23	4.06
10_Myricetin	OH	OH	H	OH	H	OH	OH	OH	4.08	4.34
11_Rhamnocitrin	OH	OH	H	OMe	H	H	OH	H	4.29	4.08
12_Rutin	OGlcRha	OH	H	OH	H	H	OH	H	4.28	4.06

**Table 2.** Flavonoid and flavonoid glycoside (flavanone and flavanonol subgroups) structures and their inhibitory activity against AH1N1 neuraminidase and AH3N2 polymerase [9]

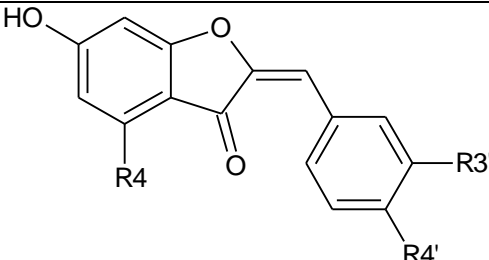


	C2	R3	R5	R7	R3'	R4'	$pIC_{50}(AH1N1)$	$pIC_{50}(AH3N2)$
13_Naringenin	$\alpha$	H	OH	OH	H	OH	4.00	4.00
14_Liquiritin	$\alpha$	H	H	OH	H	OGlc	4.00	4.00
15_Hesperidin	$\alpha$	H	OH	OGlcRha	OH	OMe	4.00	4.00
16_Catechin	$\alpha$	$\beta$ OH	OH	OH	OH	OH	4.00	4.00
17_Epicatechin	$\beta$	$\beta$ OH	OH	OH	OH	OH	4.00	4.00

**Table 3.** Isoflavonoid and aurone structures and their inhibitory activity against AH1N1 neuraminidase and AH3N2 polymerase [9]

						
	R5	R7	R3'	R4'	pIC <sub>50</sub> (H1N1)	pIC <sub>50</sub> (H3N2)
18_Daidzein	H	OH	-	OH	4.43	4.58
19_Genistein	OH	OH	-	OH	4.11	3.87
20_Formononetin	H	OH	-	OMe	4.00	4.00
21_Sophoricoside	OH	OH	-	OGlc	4.00	4.00

						
	R4	R6	R3'	R4'	pIC <sub>50</sub> (H1N1)	pIC <sub>50</sub> (H3N2)
22_Sulfuretin	H	-	OH	OH	4.53	4.56
23_Aurone	H	-	H	OH	4.66	4.66
24_Aurone	H	-	H	H	4.14	4.13
25_Aurone	OH	-	H	OH	4.59	4.65

### 2.2. Molecular modeling and conformational analysis

Flavonoid derivatives were optimized using the MM+ molecular mechanics program from the HyperChem 7.52 package [10]. The most stable conformation of a bioactive compound was obtained by conformational analysis using *Conformational Search* program from the same package. In both cases, the Polak Ribiere conjugated algorithm with a RMS gradient of 0.05 kcal/mol have been used. For conformational analysis, the variation of torsion angles and angles from the flexible rings were set at 180° and 120°, respectively. The number of cycles/optimizations was 500. All conformations having internal energy up to 4 kcal/mol above best were retained.

### 2.3. Structural descriptors

Structural descriptors for minimum energy conformations were determined using *QSAR Properties* program from HyperChem package and *PaDEL-Descriptor* ver. 2.21 free software [11]. Seven descriptors such as van der Waals molecular volume and surface, the logarithm of the octanol/water partition coefficient, logP, refractivity

or polarizability, were calculated with the *QSAR Properties*. On the other hand, 1876 descriptors were determined using *PaDEL-Descriptor* software, both 1D&2D and 3D ones (1444 and 431, respectively).

### 2.4. Quantitative structure-activity relationships (QSARs)

Classical monoparametric QSARs have been obtained using pIC<sub>50</sub> as dependent parameter and structural descriptors. First, the best models based on the highest Pearson correlation coefficient, *r*, were selected. The following QSAR model was used:

$$pIC_{50} = A(\pm errA) + B((\pm errB) \cdot P) \quad (\text{Eq. 1})$$

where *A* and *B* are the model coefficients, while *errA* and *errB* are the standard errors for coefficients. *P* stands for the structural parameter. The statistical significance of the model was evaluated through the correlation coefficient, *r*, standard deviation for the equation, *s*, and its *Fischer* value. Moreover, the validation of QSAR model was performed through cross-validation method, using the leave-half-out, LHO (odd/even), technique. All compounds were sorted in

descendent order of  $pIC_{50}$  values and models for odd and even subseries were determined. The  $pIC_{50}$  was determined in a cross technique. The validation of QSARs was obtained according to cross-validation correlation coefficient between experimental and calculated  $pIC_{50}$ ,  $q_{cv}$  or  $q^2_{cv}$ . All correlations were performed using Statistica 7.1 software (StatSoft, Inc., Tulsa, OK, USA).

### 2.5. Molecular docking

Docking of flavonoid derivatives into the enzyme receptor site was performed using the same  $MM+$  program from HyperChem, with Polak Ribiere gradient algorithm. The structures of AH1N1 and SARS-CoV-2 enzymes were taken from Protein Data Bank (PDB). They were complexed with similar standard compounds such as (1*S*,2*R*,4*S*,6*R*)-4-[[[(1*S*,2*R*)-2-clorociclohexil]metil]-2-(hidroxi-metil)-6-nitrociclohexan-1-ol for AH1N1 polymerase and the flavonoid baicalein (5,6,7-trihydroxy-2-phenyl-4*H*-1-benzopyran-4-one) for SARS-CoV-2 CL3 protease [8,12]. The most stable conformations of the studied flavonoids were oriented in the receptor site according to the orientation of the above-mentioned standard compounds. Further, the enzyme-flavonoid complex was optimized using the  $MM+$  program. The receptor-flavonoid interaction energy was

determined as the difference between the sum of internal energies for enzyme and flavonoid as separated components and the internal energy of the optimized complex. If this interaction energy was positive, the interaction was considered favorable. Only the differences between interaction energies of various enzyme-flavonoid complexes in the same interaction type were considered and evaluated. This is due to the expression of internal energies by  $MM+$ , which are arbitrary values in kcal/mol.

## 3. Results and Discussion

### 3.1. Molecular modeling and QSARs for AH1N1 and AH3N2

Molecular modeling and conformational analysis of flavonoid derivatives allow to determine the most stable conformers. These were used both for descriptor calculus and molecular docking experiments. Almost all flavonoid derivatives had planar conformations as a result of extended conjugation of benzopyrane or benzofurane rings and the phenyl substituent. Some flavonoids have not extended conjugation due to the lack of C2-C3 double bond. Flavonoid glycosides have a planar conformation of the aglycone, while the saccharide moieties had “chair” conformations. Examples of such stable conformations are presented in Figure 1.

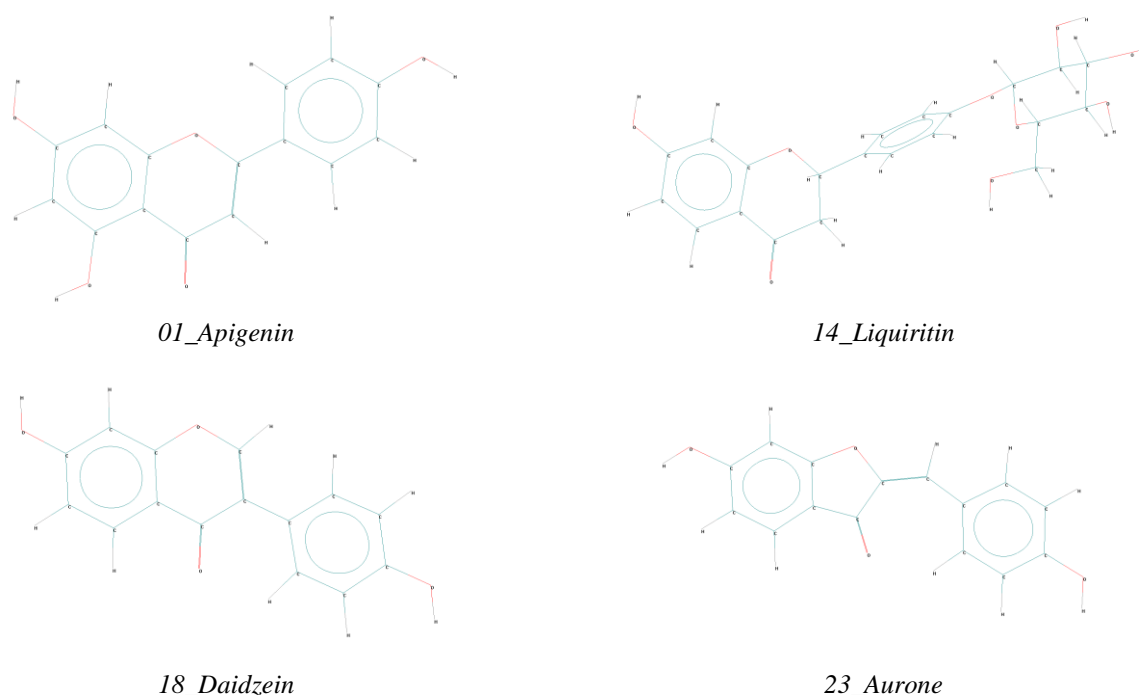


**Figure 1.** Examples of the most stable conformations for the studied flavonoids

QSAR Descriptor values were in the range of 229-545 Å<sup>2</sup> for the molecular surface and 208-477 Å<sup>3</sup> for the molecular volume. LogP values indicated that some compounds were more hydrophilic (especially flavonoid glycosides such as rutin and hesperidin), while other ones were more hydrophobic (e.g., flavanonols and aurones). They were in the range of -1.61 to 2.16. Other descriptors were the hydration energy, refractivity and polarizability, with values in the range of -44.01 ÷ -12.17 kcal/mol, 68.74-138.73 Å<sup>3</sup> and 25.99-54.75 Å<sup>3</sup>, respectively. A high number of *PaDEL* descriptors from 1D&2D and 3D subsets were calculated, most of them being intercorrelated. However, the best results for inhibitory activity against enzymes responsible for virus replication were obtained for 2D average Broto-Moreau autocorrelation descriptors and 3D topological distance based autocorrelation descriptors (Table 4). Among these, descriptors that count the carbon

atoms bound to two other carbons or the ratio of total conventional bond order with total path count from the 2D subset, as well as descriptors related to the component accessibility directional WHIM index / unweighted or weighted by relative I-state from the 3D subsets were also important.

The best QSAR models for the inhibitory activity against AH1N1 neuraminidase was obtained for *AATS6v* descriptor, with a correlation coefficient of  $r = 0.792$  and a cross-validation coefficient of  $q_{cv} = 0.755$  (Eq. 2). According to this model, the most active compound is 23\_aurone, which has a calculated  $pIC_{50}$  of 4.52, very close to the experimental value.

$$pIC_{50(H1N1)} = 2.34(\pm 0.31) + 0.0098(\pm 0.0016) \cdot AATS6v \quad (\text{Eq. 2})$$

$n=25, r=0.792, q_{cv}=0.755, s=0.13, F=38.8$

**Table 4.** Values of the structural descriptors\* having the highest influence on the enzymatic inhibition effect

Compound	<i>AATS6v</i>	<i>TDB5m</i> **	<i>TDB6m</i> **
01_Apigenin	77.7	364.9	500.8
02_Luteolin	81.3	383.6	525.9
03_Dinatin	68.3	361.8	436.3
04_Scutellarin	77.8	396.4	500.7
05_Galuteolin	79.8	380.2	479.8
06_Vitexin	80.0	367.5	478.1
07_Chrysin	69.7	365.0	449.3
08_Kaempferol	72.5	-	-
09_Quercetin	78.2	-	-
10_Myricetin	81.9	-	-
11_Rhamnocitrin	68.7	-	-
12_Rutin	80.6	342.6	461.7
13_Naringenin	64.0	306.7	415.5
14_Liquiritin	60.1	299.6	375.3
15_Hesperidin	66.7	293.0	402.5
16_Catechin	57.6	314.0	364.2
17_Epicatechin	57.6	300.4	331.9
18_Daidzein	73.4	362.7	468.3
19_Genistein	75.9	371.5	479.0
20_Formononetin	63.5	314.1	405.1
21_Sophoricoside	63.7	329.0	391.6
22_Sulfuretin	85.1	393.6	544.2
23_Aurone	80.4	397.6	507.1
24_Aurone	77.0	400.0	483.1
25_Aurone	80.0	441.5	507.5

\* *AATS6v* – Average Broto-Moreau autocorrelation - lag 6 / weighted by van der Waals volumes

*TDB5m* – 3D topological distance based autocorrelation - lag 5 / weighted by mass

*TDB6m* – 3D topological distance based autocorrelation - lag 6 / weighted by mass

\*\* 3D descriptors cannot be calculated for 3-OH substituted flavonoids.



If the TDB6m 3D descriptor is used for the QSAR model, the correlation coefficient is higher ( $r=0.838$ ) as well as the cross-validation coefficient ( $q_{cv}=0.827$ ) (Eq. 3). On the other hand, a similar descriptor was the most important for the AH3N2 polymerase inhibitory activity, with an  $r=0.714$  and  $q_{cv}=0.680$  (Eq. 4). According to these equations, the most active compounds are 22\_Sulfuretin (an aurone) and 25\_Aurone, respectively (calculated  $pIC_{50}$  of 4.58 and 4.68). As a partial conclusion, the most active class of flavonoid derivatives against AH1N1 and AH3N2 enzymes are aurones, which were mainly considered in the ligand-receptor docking experiments, for both AH1N1 and SARS-CoV-2 cases.

$$pIC_{50(AH1N1)} = 2.78(\pm 0.22) + 0.0033(\pm 0.0005) \cdot TDB6m \quad (\text{Eq. 3})$$

$$n=21, r=0.838, q_{cv}=0.827, s=0.13, F=45.0$$

$$pIC_{50(AH3N2)} = 2.56(\pm 0.39) + 0.0048(\pm 0.0011) \cdot TDB5m \quad (\text{Eq. 4})$$

$$n=21, r=0.714, q_{cv}=0.680, s=0.20, F=19.8$$

### 3.2. Molecular docking of flavonoid derivatives in the AH1N1 and SARS-CoV-2 receptor sites

The most active compounds in the class of flavonoids and similar derivatives for inhibiting neuraminidase enzymes involved in the replication / functionality of AH1N1 and AH3N2 viruses were evaluated for their interaction with other AH1N1 and the recent SARS-CoV-2 viruses (polymerase and protease, respectively). The reference compounds co-crystallized with these receptors, whose enzyme complexes were determined by X-ray diffractometry [8,12], allowing the identification of the three-dimensional structure of the receptor, were replaced by the active compounds 01\_Apigenin and 23\_Aurone and, for comparison, and with the less active compound 09\_Quercetin. The optimization of the complexes was achieved by *MM* + molecular mechanics and thus the stable Ligand-Receptor complexes were obtained, for which the interaction energies were determined (Figures 2 and 3). Similarly, the most active compound “23\_Aurone” with the SARS-CoV-2 proteinase receptor was similarly complexed and evaluated for molecular identification to identify the possibility of using such aurone compounds to inhibit SARS-CoV-2 replication that led to the COVID-19 pandemic (Figure 4). It was observed

that the interaction energies were positive in all cases (efficient interaction), with maximum values for the most active compounds in the case of AH1N1 Ligand-Receptor complexes for 23\_Aurone, followed by 01\_Apigenin (an interaction energy with only 0.8 kcal/mol lower). A positive value of the interaction energy was also obtained for the 23\_Aurone – SARS-CoV-2 Receptor complex, which indicates a possible inhibitory activity by such aurone compounds of the replication of this new virus.

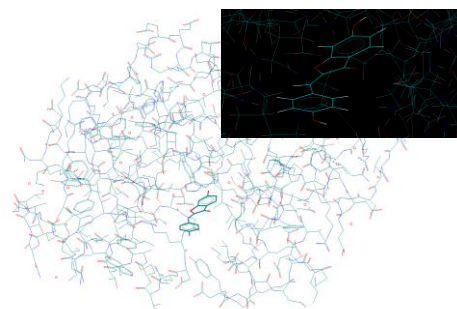


**Figure 2.** The optimized complex of 23\_Aurone and AH1N1 polymerase (3D structure based on XRD from [8]). The detail of the interaction site is presented in the right corner

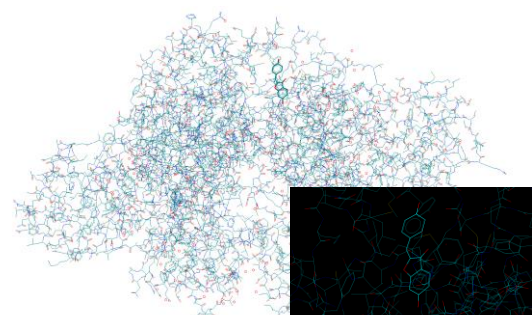


**Figure 3.** The optimized complex of 23\_Aurone and SARS-CoV-2 3CL protease (3D structure based on XRD from [12]). The detail of the interaction site is presented in the right corner

## 4. Conclusion

Twenty-five flavonoid compounds and standard compounds with activity against the replication of influenza AH1N1 and AH3N2 viruses were selected from the literature. Stable conformations showed planar structures for aurones, which reveals the highest interaction energies both with AH1N1 polymerases and SARS-CoV-2 proteases. This observation indicates a possible inhibitory activity of such aurone derivatives against the replication of this new virus.

**Acknowledgments.** The author wants to thank S. Funar-Timofei and M. Mracec (“Coriolan Drăgulescu” Institute of Chemistry, Romanian Academy) for the help with Statistica 7.1 and HyperChem packages. The author also wants to thank M.M. Puiu for the contribution to molecular modeling of flavonoid derivatives.

**Compliance with Ethics Requirements.** The author declares that he respect the journal’s ethics requirements. The author declares that he has no conflict of interest.

## References

- [1] Sullivan, S.J.; Jacobson, R.M.; Dowdle, W.R.; Poland, G.A., 2009 H1N1 Influenza, *Mayo. Clin. Proc.* **2010**, 85(1), 64-76, <https://doi.org/10.4065/mcp.2009.0588>
- [2] Du, Q.-S.; Wang, S.-Q.; Huang, R.B.; Chou, K.-C., Computational 3D structures of drug-targeting proteins in the 2009-H1N1 influenza A virus, *Chemical Physics Letters* **2010**, 485, 191-195, <https://doi.org/10.1016/j.cplett.2009.12.037>
- [3] González-Parra, G.; Arenas, A.J.; Aranda, D.F.; Segovia, L., Modeling the epidemic waves of AH1N1/09 influenza around the world, *Spatial and Spatio-temporal Epidemiology* **2011**, 2, 219-226, <https://doi.org/10.1016/j.sste.2011.05.002>
- [4] Girard, M.P.; Tam, J.S.; Assossou, O.M.; Kieny, M.P., The 2009 A (H1N1) influenza virus pandemic: A review, *Vaccine* **2010**, 28, 4895-4902, <https://doi.org/10.1016/j.vaccine.2010.05.031>
- [5] Scalera, N.M.; Mossad, S.B., The First Pandemic of the 21st Century: Review of the 2009 Pandemic Variant Influenza A (H1N1) Virus, *Postgraduate Medicine* **2009**, 121(5), 43-47, <http://dx.doi.org/10.3810/pgm.2009.09.2051>
- [6] Liu, C.; Zhou, Q.; Li, Y.; Garner, L.V.; Watkins, S.P.; Carter, L.J.; Smoot, J.; Gregg, A.C.; Daniels, A.D.; Jervey, S.; Albaiu, D., Research and development on therapeutic agents and vaccines for COVID-19 and related human coronavirus diseases, *ACS Central Science* **2020**, 6(3), 315-331, <https://dx.doi.org/10.1021/acscentsci.0c00272>
- [7] Sohrabi, C.; Alsafi, Z.; O’Neill, N.; Khan, M.; Kerwan, A.; Al-Jabir, A.; Iosifidis, C.; Agha, R., World Health Organization declares global emergency: A review of the 2019 novel coronavirus (COVID-19), *International Journal of Surgery* **2020**, 76, 71-76, <https://doi.org/10.1016/j.ijisu.2020.02.034>
- [8] Fudo, S.; Yamamoto, N.; Nukaga, M.; Odagiri, T.; Tashiro, M.; Hoshino, T., Endonuclease inhibitor 1 bound to influenza strain H1N1 polymerase acidic subunit N-terminal region at pH 7.0, *PDB Protein Data Bank* **2015**, <https://doi.org/10.2210/pdb5FDD/pdb>
- [9] Liu, A.-L.; Wang, H.-D.; Lee, S.M.Y.; Wang, Y.-T.; Du, G.-H., Structure–activity relationship of flavonoids as influenza virus neuraminidase inhibitors and their in vitro anti-viral activities, *Bioorganic & Medicinal Chemistry* **2008**, 16, 7141-7147, <https://doi.org/10.1016/j.bmc.2008.06.049>
- [10] HyperChem, version 7.52, **2005**, Hypercube, Inc., Gainesville, FL, USA
- [11] Yap, C.W., PaDEL-Descriptor: An open source software to calculate molecular descriptors and fingerprints, *Journal of Computational Chemistry* **2011**, 32(7), 1466-1474
- [12] Su, H.X., Zhao, W.F., Li, M.J., Xie, H., Xu, Y.C., SARS-CoV-2 3CL protease (3CL pro) in complex with a novel inhibitor, *PDB Protein Data Bank* **2020**, <https://doi.org/10.2210/pdb6M2N/pdb>